Article

Insights into the Recognition and Association of Transmembrane □-Helices. The Free Energy of □-Helix Dimerization in Glycophorin A

Jrme Hnin, Andrew Pohorille, and Christophe Chipot

J. Am. Chem. Soc., **2005**, 127 (23), 8478-8484• DOI: 10.1021/ja050581y • Publication Date (Web): 19 May 2005

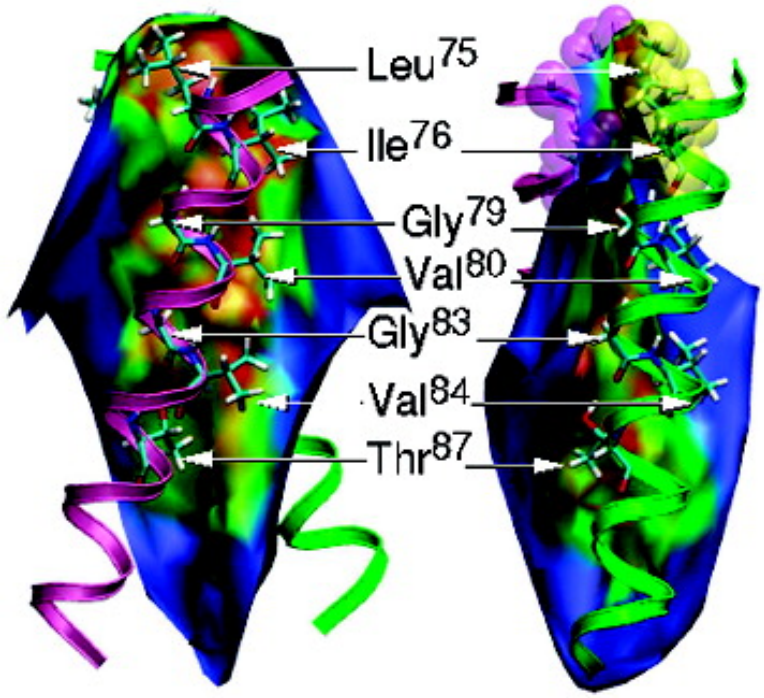

More About This Article

Additional resources and features associated with this article are available within the HTML version:

- Supporting Information
- Links to the 7 articles that cite this article, as of the time of this article download
- Access to high resolution figures
- Links to articles and content related to this article
- Copyright permission to reproduce figures and/or text from this article

J|A|C|S
ARTICLES
Published on Web 05/19/2005

Insights into the Recognition and Association of Transmembrane α-Helices. The Free Energy of α-Helix Dimerization in Glycophorin A

Jérôme Hénin,[†] Andrew Pohorille,[‡] and Christophe Chipot*,[†]

Contribution from the Equipe de dynamique des assemblages membranaires, UMR CNRS/UHP 7565, Institut nancéien de chimie moléculaire, Université Henri Poincaré, BP 239, 54506 Vandoeuvre-lès-Nancy Cedex, France, and NASA Ames Research Center, Exobiology Branch, Mail stop 239-4, Moffett Field, California, 94035-1000

Received January 28, 2005; E-mail: Christophe.Chipot@edam.uhp-nancy.fr

Abstract: The free energy of α-helix dimerization of the transmembrane (TM) region of glycophorin A was estimated from a 125-ns molecular dynamics (MD) simulation in a membrane mimetic. The free energy profile was obtained by allowing the TM helical segments to diffuse reversibly along the reaction pathway. Partition of the potential of mean force into free energy components illuminates the critical steps of α-helix recognition and association. At large separations, the TM segments are pushed together by the solvent, allowing initial, but not necessarily native, interhelical interactions to occur. This early recognition stage precedes the formation of native contacts, which is accompanied by a tilt of the helices, characteristic of the dimeric structure. This step is primarily driven by the van der Waals helix−helix interactions. Free energy perturbation calculations of the L75A and I76A point mutations reveal a disruption in helix−helix association due to a loss of favorable dispersion interactions. Additional MD simulations of the native TM dimer and of a single α-helix confirm that, prior to association, individual α-helices are independently stable, in agreement with the "two-stage" model of integral membrane protein folding.

Introduction

Although membrane proteins can be exceedingly complex, their transmembrane (TM) regions are often relatively simple. Commonly, they consist of a bundle of integral α-helices or a barrel of β-strands.[1−3] A convenient framework for understanding how the TM regions are formed is provided by the "two-stage" model.[4−6] According to this model, elements of the secondary structure, most often α-helices, are first formed and inserted into the bilayer. This is followed by specific interactions of the helices, resulting in higher-order, native structures. Since the original "two-stage" model is not sufficient to encompass all membrane proteins, it has been recently extended to account for ligand binding, folding of extra-membranous loops, insertion of peripheral domains, and the formation of quaternary structures.[7] Yet, the cornerstone of the whole process (i.e., the interactions that drive recognition and association of TM α-helices) still remains only partially understood. A successful strategy to probe these interactions is to study simple models composed of a few TM peptides. The relevance of these models is underscored by the fact that some membrane proteins can retain their main functionalities even if a large fraction of the protein has been removed.[2,8,9] Furthermore, some very simple membrane proteins have been shown to aggregate spontaneously and form sequence-dependent, functional complexes.[8,10−14]

An excellent system to study helix−helix recognition is the dimeric TM domain of glycophorin A (GpA).[15−18] GpA, a glycoprotein ubiquitous to the human erythrocyte membrane, forms noncovalent dimers through the reversible association of its membrane-spanning domain.[19,20] This region consists of residues 62−101, but only 24 of them, residues 73 to 96, actually adopt an α-helical conformation.[17] On the basis of thorough random mutagenesis, a model of the GpA TM dimer

[†] Université Henri Poincaré.
[‡] NASA Ames Research Center.

(1) Montal, M. *Curr. Opin. Struct. Biol.* **1995**, *5*, 501−506.
(2) Montal, M. *Annu. Rev. Biophys. Biomol. Struct.* **1995**, *24*, 31−57.
(3) Bayley, H. *Curr. Opin. Biotechnol.* **1999**, *10*, 94−103.
(4) Engelman, D.; Steitz, T. A. *Cell* **1981**, *23*, 411−422.
(5) Popot, J. L.; Engelman, D. M. *Biochemistry* **1990**, *29*, 4031−4037.
(6) Popot, J. L.; Engelman, D. M. *Annu. Rev. Biochem.* **2000**, *69*, 881−922.
(7) Engelman, D.; Chen, Y.; Chin, C. N.; Curran, A. R.; Dixon, A. M.; Dupuy, A. D.; Lee, A. S.; Lehnert, U.; Matthews, E. E.; Reshetnyak, Y. K.; Senes, A.; Popot, J. L. *FEBS Lett.* **2003**, *555*, 122−125.
(8) Duff, K. C.; Ashley, R. H. *Virology* **1992**, *190*, 485−489.
(9) Oblatt-Montal, M.; Buhler, L.; Iwamoto, T.; Tomich, J.; Montal, M. *J. Biol. Chem.* **1993**, *268*, 14601−14607.
(10) Lear, J. D.; Wasserman, Z. R.; DeGrado, W. F. *Science* **1988**, *240*, 1177−1181.
(11) Åkerfeldt, K. S.; Lear, J. D.; Wasserman, Z. R.; Chung, L. A.; DeGrado, W. F. *Acc. Chem. Res.* **1993**, *26*, 191−197.
(12) Cafiso, D. S. *Annu. Rev. Biophys. Biomol. Struct.* **1994**, *23*, 141−165.
(13) Bechinger, B. *J. Membr. Biol.* **1997**, *156*, 197−211.
(14) Duclohier, H.; Wroblewski, H. *J. Membr. Biol.* **2001**, *184*, 1−12.
(15) Lemmon, M. A.; Flanagan, J.; Hunt, J.; Adair, B.; Bormann, B. J.; Dempsey, C.; Engelman, D. M. *J. Biol. Chem.* **1992**, *267*, 7683−7689.
(16) Treutlein, H. R.; Lemmon, M. A.; Engelman, D. M.; Brünger, A. T. *Biochemistry* **1992**, *31*, 12726−12732.
(17) MacKenzie, K. R.; Prestegard, J. H.; Engelman, D. M. *Science* **1997**, *276*, 131−133.
(18) MacKenzie, K. R.; Engelman, D. M. *Proc. Natl. Acad. Sci. U.S.A.* **1998**, *95*, 3583−3590.
(19) Bormann, B. J.; Knowles, W. J.; Marchesi, V. T. *J. Biol. Chem.* **1989**, *264*, 4033−4037.
(20) Lemmon, M. A.; Flanagan, J.; Treutlein, H. R.; Zhang, J.; Engelman, D. M. *Biochemistry* **1992**, *31*, 12719−12725.

10.1021/ja050581y CCC: $30.25

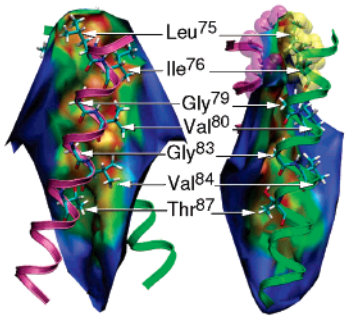

A

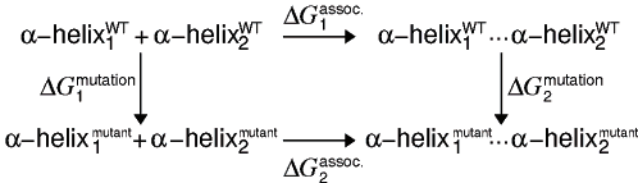

B

Figure 1. (A) Helix−helix interface of the GpA TM domain. The color scale varying from blue to red reflects decreasing interhelical distances. The heptad of amino acids involved in helix−helix association is highlighted, and the two residues chosen for the point mutations, viz. replacement of Leu75 and Ile76 by alanine, are featured as van der Waals spheres. Image rendering was obtained with VMD.[27] (B) Thermodynamic cycle describing the L75A and I76A point mutations in the TM domain of GpA. The vertical legs correspond to "alchemical transformations" in a single α-helix and in the helix homodimer. The dissociation free energy estimated for the WT corresponds to $-\Delta G_1^{\text{assoc}}$. Closure of the thermodynamic cycle implies that $\Delta G_2^{\text{mutation}} - \Delta G_1^{\text{mutation}} = \Delta G_2^{\text{assoc}} - \Delta G_1^{\text{assoc}}$.

has been proposed, in which helix−helix association is promoted by the specific interactions of seven residues located on one face of each α-helix[15,16,21,22] (Figure 1). This model has been confirmed by nuclear magnetic resonance (NMR) spectroscopy in detergent micelles.[17] It was further shown in this study that the α-helices formed by residues 73−96 interact at a right-handed, 40° crossing angle. In addition to structural information, a variety of thermodynamic data are also available for GpA. In particular, the free energy of helix−helix dissociation in detergent micelles has been measured for the wild type (WT),[23,24] and the effects of single-point mutations of key residues on the stability of the dimer have been probed.[25,26]

In principle, important additional insight into the factors that influence helix−helix association can be gained from computer simulations, provided that the latter are sufficiently reliable. Thus far, however, accuracy of such simulations has not been tested. Structural and thermodynamic data available for GpA are very well-suited for such a test. Here, we report molecular dynamics (MD) simulations of this system that yield results of accuracy comparable with those obtained from experiments. In particular, we present the first calculations of the free energy profile associated with the reversible dissociation of a membrane protein and show how the dimerization free energy depends on helix−helix and helix−solvent interactions. We further discuss the free energy changes caused by mutations of two residues, Leu75 and Ile76 (see Figure 1), which are essential for efficient interhelical packing. This information is of paramount interest,[26] but admittedly cannot be accessed experimentally.

Methods

Description of the Model. The TM region of GpA, corresponding to the sequence ITLIIFGVMAGVIGTILLISYGI, that is, residues 73−95, blocked at the N- and C-termini by Ac− and −NHMe groups, was used to investigate α-helix dimerization.[28] The environment consisted of a lamella of dodecane in equilibrium between two lamellae of water. The dimensions of the system in the plane of the water−dodecane interfaces were 50 × 50 Å^2. The width of the dodecane layer was approximately equal to that of the hydrophobic core of a palmitoyloleylphosphatidylcholine (POPC) bilayer. The helix dimer was first inserted into the dodecane layer, and overlapping dodecane molecules were deleted. After a short energy minimization, an equilibration MD simulation was performed in which temperature was increasing slowly until it reached the target value of 300 K.

The choice of dodecane as a membrane mimetic was dictated by the slow relaxation times of collective motions in phospholipid bilayers, compared to typical lengths of MD trajectories.[29] Similar limitations apply to detergent micelles, although detergents can be utilized to model micellar aggregation around preformed protein assemblies.[30,31] Although a membrane mimetic is not always an appropriate environment for many membrane proteins, it appears to be so for GpA. In fact, most experiments on this system were carried out not in bilayers but in detergent micelles,[23−25] and the results were similar for detergents of different nature. In addition, the dimer structure determined from NMR in micelles and in phospholipid membranes was also quite similar,[17,18,28] albeit small differences in the crossing angle were noted. More generally, it has been suggested that specifics of the hydrophobic environment do not play a major role in stabilizing helix association.[6]

Molecular Dynamics Simulations. All MD simulations were performed using the program NAMD[32,33] with the CHARMM27 force field[34] and the TIP3P water model. The equations of motion were integrated using the multiple time step Verlet r-RESPA algorithm with a time step of 2 fs. Covalent bonds between heavy and hydrogen atoms were constrained using SHAKE/RATTLE, except for water, for which the SETTLE algorithm was applied. Dimensions of the periodic box in the plane of the interfaces were kept fixed to 50 × 50 Å^2.

The temperature and the normal pressure were maintained, respectively, at 300 K and 1 bar, using Langevin dynamics and the Langevin piston method. Long-range electrostatic forces were included using the particle-mesh Ewald approach.

Free Energy Calculations. To investigate dimerization of GpA, the reaction coordinate, ξ, was chosen as the distance separating the centers of mass of the two α-helices. The free energy changes along ξ were

(21) Lemmon, M. A.; Treutlein, H. R.; Adams, P. D.; Brünger, A. T.; Engelman, D. M. *Nat. Struct. Biol.* **1994**, *1*, 157−163.
(22) Adams, P. D.; Engelman, D. M.; Brünger, A. T. *Proteins: Struct., Funct., Genet.* **1996**, *26*, 257−261.
(23) Fisher, L. E.; Engelman, D. M.; Sturgis, J. N. *J. Mol. Biol.* **1999**, *293*, 639−651.
(24) Fisher, L. E.; Engelman, D. M.; Sturgis, J. N. *Biophys. J.* **2003**, *85*, 3097−3105.
(25) Fleming, K. G.; Ackerman, A. L.; Engelman, D. M. *J. Mol. Biol.* **1997**, *272*, 266−275.
(26) Fleming, K. G. *J. Mol. Biol.* **2002**, *323*, 563−571.
(27) Humphrey, W.; Dalke, A.; Schulten, K. *J. Mol. Graphics* **1996**, *14*, 33−38.
(28) Smith, S. O.; Song, D.; Shekar, S.; Groesbeek, M.; Ziliox, M.; Aimoto, S. *Biochemistry* **2001**, *40*, 6553−6558.
(29) Stockner, T.; Ash, W. L.; MacCallum, J. L.; Tieleman, D. P. *Biophys. J.* **2004**, *87*, 1650−1656.
(30) Braun, R.; Engelman, D. M.; Schulten, K. *Biophys. J.* **2004**, *87*, 754−763.
(31) Bond, P. J.; Cuthbertson, J. M.; Deol, S. S.; Sansom, M. S. P. *J. Am. Chem. Soc.* **2004**, *126*, 15948−15949.
(32) Kalé, L.; Skeel, R.; Bhandarkar, M.; Brunner, R.; Gursoy, A.; Krawetz, N.; Phillips, J.; Shinozaki, A.; Varadarajan, K.; Schulten, K. *J. Comput. Phys.* **1999**, *151*, 283−312.
(33) Bhandarkar, M. et al. *NAMD users guide*, version 2.5; Theoretical biophysics group, University of Illinois and Beckman Institute: Urbana, IL, 2003.
(34) MacKerell, A. D., Jr. et al. *J. Phys. Chem. B* **1998**, *102*, 3586−3616.

estimated using the adaptive biasing force (ABF) method,[35] which relies upon the integration of the average force acting on ξ, obtained from unconstrained MD simulations.[36] In the course of the simulation, a biasing force is estimated such that, once applied to the system, it yields a Hamiltonian in which no average force acts along ξ. As a result, all values of ξ are sampled with the same probability, which, in turn, greatly improves the accuracy of the calculated free energies. In contrast with probability-based methods, such as adaptive umbrella sampling,[37,38] the present approach uses a purely local estimate of the free energy derivative, so that the biasing force is updated continuously. To gain additional efficiency, the pathway joining the bound dimer and the dissociated helices, viz. $6 \leq \xi \leq 25$ Å, was divided into 10 windows. For each window, up to 15 ns of MD trajectory was generated. Instantaneous values of the force were accrued in bins 0.1 Å wide. The standard error of the free energy difference was estimated using the expression given by Rodriguez-Gomez et al.[39]

The free energy changes due to mutations of Leu75 and Ile76 to alanine were obtained from the thermodynamic cycle shown in Figure 1. These "alchemical transformations" were performed using the dual-topology paradigm,[40] wherein the initial state and the final state are defined by means of distinct, noninteracting topologies. The free energy perturbation (FEP) approach[41] was employed to scale the interactions of the transformed moieties with their environment by means of a linear parameter, λ. For each transformation shown in Figure 1, 50 states corresponding to different values of λ were simulated for 100 ps, following 20 ps of equilibration. This corresponds to a total simulation length of 6 ns for each leg of the thermodynamic cycle. Assuming that each free energy difference computed at a given λ-state constitutes an independent observable, the error was determined using a first-order approximation, in which the change in the Gibbs free energy between two intermediate states is expressed as:

$$\Delta G = -\frac{1}{\beta}\left\{\ln\langle\exp[-\beta\Delta\mathcal{V}(\boldsymbol{x};\lambda)]\rangle_\lambda \pm \frac{\delta\epsilon}{\langle\exp[-\beta\Delta\mathcal{V}(\boldsymbol{x};\lambda)]\rangle_\lambda}\right\} \quad (1)$$

$\beta \equiv 1/k_B T$, where k_B is the Boltzmann constant and T is the temperature. $\mathcal{V}(\boldsymbol{x};\lambda)$ is the potential energy of the system, $\boldsymbol{x}$ is the function of the Cartesian coordinates, and λ is the coupling parameter. $\delta\epsilon$ is the statistical error on the ensemble average, $\langle\exp[-\beta\Delta\mathcal{V}(\boldsymbol{x};\lambda)]\rangle_\lambda$, defined as:

$$\delta\epsilon^2 = \frac{1+2\tau}{N}\{\langle\exp[-2\beta\Delta\mathcal{V}(\boldsymbol{x};\lambda)]\rangle_\lambda - \langle\exp[-\beta\Delta\mathcal{V}(\boldsymbol{x};\lambda)]\rangle_\lambda^2\} \quad (2)$$

Here, N is the number of samples accrued in the FEP calculation, and $(1 + 2\tau)$ is the sampling ratio of the latter.[42]

Results and Discussion

Dynamics of a Single Transmembrane α-Helix and the Dimer. As a preamble to the investigation of the dissociation of the dimeric TM domain of GpA, two separate simulations were performed, in which either a single TM GpA α-helix or the TM dimer were placed in the water−dodecane environment. These two systems correspond to the endpoints of the dimerization process. For each system, a 15-ns MD trajectory was generated. The purpose of these simulations was to establish the stability of each system and to compare the structure of the dimer with that determined experimentally.[17,18,28] This initial step offers a basis for assessing the accuracy of the simulation parameters utilized.

In the simulation involving the single TM segment, the equilibrated α-helix was initially placed across the dodecane lamella, with the Ac− and −NHMe blocking groups extending into the water−hydrocarbon interface. In its preferred orientation, the helical segment is nearly perpendicular to the water−dodecane interface (i.e., tilted by ca. 12°). Alignment of the longitudinal axis of the α-helix with the normal to the interface corresponds to an increase of the free energy equal to ca. 1 kcal/mol, indicating unhindered reorientation in the range of ca. ±10°. As shown in Figure 2, the distance root-mean-square deviation (RMSD) of the backbone atoms with respect to the initial structure rarely exceeded 2.4 Å, mostly due to slight fraying at the N- and C-termini. No significant perturbations of the α-helical core were observed. This suggests that the single TM segment of GpA is a stable, independently folded entity, as implied by the "two-stage" model.[4−6]

The simulation of the dimer reveals a different orientation of the two helical segments, as depicted in Figure 2. The angular distributions of the individual α-helices with respect to the interface normal are symmetric and, on average, equal to 22°. The crossing angle between the helices, defined as the angle formed by the two longitudinal axes, fluctuates about the average value of 44°, in close agreement with the 40° estimates from NMR experiments[17,18,28] and with the crossing angle calculated from 1-ns MD simulations of the dimer in a variety of lipid bilayers.[44]

The position of the dimer along the direction normal to the dodecane lamella varies by about 1.5 Å in the first 5 ns of simulated time, after which it remains stable, fluctuating with a standard deviation of 0.65 Å. Compared to the free monomer, the dimer exhibits somewhat smaller conformational fluctuations, as measured by the total distance RMSD, which plateaus at 2.0 Å. As shown in Figure 2, the core of each TM segment remains perfectly α-helical, indicating that the secondary structure of the dimer is preserved in the water−dodecane lamellar system. The simulation also shows that the two TM helices are strongly bound by means of key interhelical interactions. Analysis of protein−protein contacts highlights well-conserved pairs of interacting residues, especially between Val80 and Gly79 or Gly83 and between the symmetry-related Gly79. All these interactions are in the GxxxG motif[45] that contributes to the stability of the helix dimer,[18] albeit it appears to be neither necessary nor sufficient for dimerization.[46] The contacts correspond to the formation of nonconventional hydrogen bonds, in which the hydrogen atom of the two C_α−H bonds of glycine acts as a donor.[47] The energy of a C_α−H···O bond was estimated in quantum-mechanical calculations to be on the order of 2.5−3.0 kcal/mol, approximately one-half of a conventional N−H···O hydrogen bond. In addition to the contacts involved in the GxxxG motif, the MD simulation reveals a strong interaction between Val84 and Gly83 and between the symmetry-related Thr87. The latter also interacts

(35) Darve, E.; Pohorille, A. *J. Chem. Phys.* **2001**, *115*, 9169−9183.
(36) Hénin, J.; Chipot, C. *J. Chem. Phys.* **2004**, *121*, 2904−2914.
(37) Bartels, C.; Karplus, M. *J. Comput. Chem.* **1997**, *18*, 1450−1462.
(38) Bartels, C.; Karplus, M. *J. Phys. Chem. B* **1998**, *102*, 865−880.
(39) Rodriguez-Gomez, D.; Darve, E.; Pohorille, A. *J. Chem. Phys.* **2004**, *120*, 3563−3570.
(40) Pearlman, D. A. *J. Phys. Chem.* **1994**, *98*, 1487−1493.
(41) Zwanzig, R. W. *J. Chem. Phys.* **1954**, *22*, 1420−1426.
(42) Straatsma, T. P.; Berendsen, H. J. C.; Stam, A. J. *Mol. Phys.* **1986**, *57*, 89−95.
(43) Frishman, D.; Argos, P. *Proteins: Struct., Funct., Genet.* **1995**, *23*, 566−579.
(44) Petrache, H. I.; Grossfield, A.; MacKenzie, K. R.; Engelman, D. M.; Woolf, T. B. *J. Mol. Biol.* **2000**, *302*, 727−746.
(45) Russ, W. P.; Engelman, D. M. *J. Mol. Biol.* **2000**, *296*, 911−919.
(46) Doura, A. K.; Fleming, K. G. *J. Mol. Biol.* **2004**, *343*, 1487−1497.
(47) Senes, A.; Ubarretxena-Belandia, I.; Engelman, D. M. *Proc. Natl. Acad. Sci. U.S.A.* **2001**, *98*, 9056−9061.

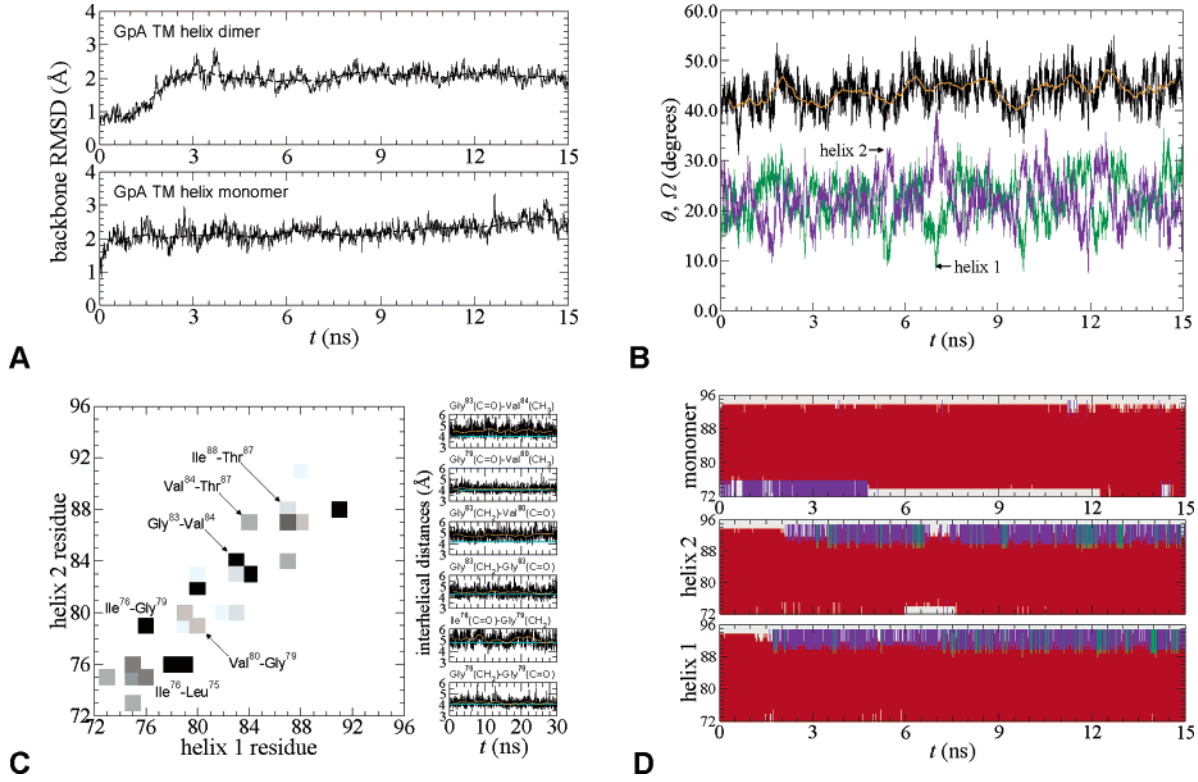

Figure 2. (A) Distance RMSD of the GpA α-helix dimer (above) and of a single α-helical segment, evaluated using backbone atoms only. (B) Time evolution of the crossing angle formed by the longitudinal axis of the two α-helices forming the TM domain of GpA. The running average is shown in orange, and the orientation of the individual segments with respect to the normal to the aqueous interface are displayed in green and purple. (C) Two-dimensional plot of the key interactions in the GpA α-helix dimer, averaged over an MD trajectory of 15 ns (left). Darker squares denote interactions persisting over longer times. Comparison of remarkable interhelical distances obtained from the MD trajectory (black solid line with running averages in orange) and from solid-state NMR measurements (straight cyan line).[28] (D) Secondary structure analysis[43] of the TM domain of GpA as a function of time. α-Helices, π-helices, turns, and coils are shown, respectively, in red, green, purple, and gray. For comparison, evolution of the secondary structure of a single α-helix (monomer) has been included.

with both the backbone and the side chain of Val84 via its O_γ atom, as has been observed experimentally.[17,18] Other interhelical distances determined from solid-state NMR[28] are equally well-preserved. These results are summarized in Figure 2. Another quantity of interest is the solvent accessible surface area (SASA) buried at the interface between the helices. The average buried surface of 882 ± 38 Å^2, estimated over the complete MD trajectory using the Shrake and Rupley algorithm[48] with a 1.4 Å probe is in good agreement with previous estimates.[49] Put together, the agreement of the present results with experiment suggests that the choice of a water−hydrocarbon assembly to mimic a hydrated lipid bilayer or detergent micelles does not lead to any significant changes in the protein structure.

Free Energy of α-Helix Dimerization. The free energy profile characterizing the reversible dissociation of the two α-helices forming the TM region of GpA is shown in Figure 3. The minimum in the profile is located at a distance separating the centers of mass equal to 8.2 Å. This corresponds to a close packing of the helices, with interdigitations of the residues directly in contact. As the two TM segments of GpA move away from each other, helix−helix interactions, especially in the region where the two α-helices cross, are progressively disrupted. Initially, this leads to an abrupt increase of the free energy. As the separation of the α-helices further increases, the free energy profile levels off and reaches a plateau at approximately 21 Å, a distance beyond which the dimer is fully dissociated. Over the complete reaction pathway, the relative vertical position of the two TM segments spans a range of ±4 Å.

The apparent dissociation free energy can be obtained by integrating the potential of mean force (PMF) to an appropriate separation, which delineates the limit of association. In cylindrical coordinates, the association constant[50] can be written as:

$$K_a = 2\pi \int_0^{\xi_{max}} \xi \exp[-\beta G(\xi)]\, d\xi \qquad (3)$$

Here, ξ_{max} stands for the cylindrical radius separating associated and dissociated states of the two α-helices. Considering that the above integral reaches a plateau beyond 10 Å, the exact value of ξ_{max} is not critical for the assessment of K_a. Conversion of the surface K_a into a dimensionless quantity is achieved by defining a reference state compatible with experimental measurements and assuming an activity coefficient of GpA equal to 1.[24,26]

Direct comparison of the apparent dissociation free energy with experiment is difficult because analytical ultracentrifugation[25] and fluorescence resonance energy transfer[24] measurements were carried out in detergent micelles. Additionally, it has been shown that the nature and the concentration of the

(48) Shrake, A.; Rupley, J. A. *J. Mol. Biol.* **1973**, *79*, 351−371.
(49) Mingarro, I.; Elofsson, A.; von Heijne, G. *J. Mol. Biol.* **1997**, *272*, 633−641.
(50) Shoup, D.; Szabo, A. *Biophys. J.* **1982**, *40*, 33−39.

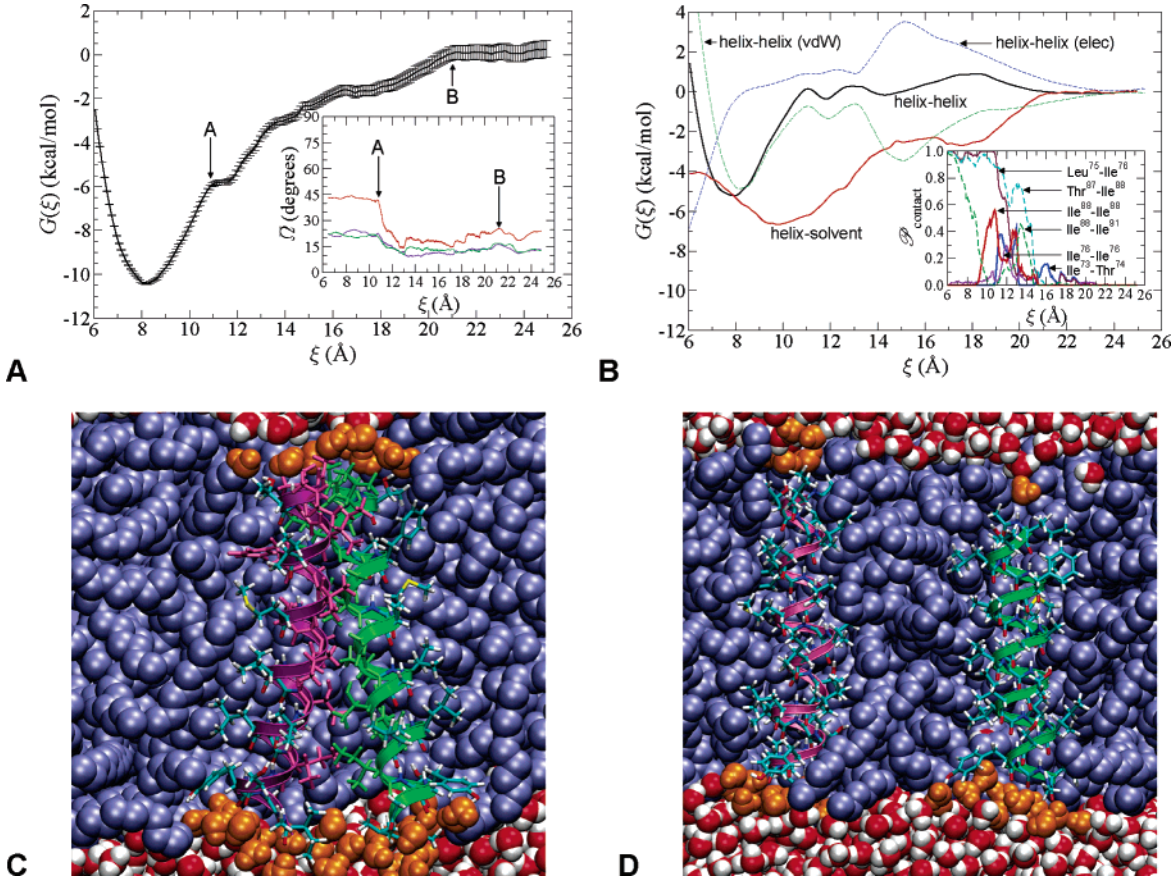

Figure 3. (A) PMF for the reversible dimerization of the TM domain of GpA. Inset: Evolution of the average interhelical crossing angle as a function of ξ (red solid line). Orientation of the individual α-helices with respect to the normal to the aqueous interface is included for comparison. Point A marks the end of the regime dominated by helix−helix interactions. Beyond point B, α-helices can be considered as noninteracting. (B) Partition of the total dissociation free energy (black solid line) into helix−helix (red dashed line) and helix−solvent (blue dotted−dashed line) contributions. Inset: Evolution of selected interhelical contact probabilities as a function of ξ. Two residues are considered to be in contact if any distance between atoms in these residues is less than 3 Å. (C) Snapshot of the α-helical dimer in its associated state, i.e., near $\xi = 8.2$ Å. (D) Snapshot of the TM α-helical dimer of GpA in the dissociated state, wherein the value of the reaction coordinate exceeds 20 Å. Individual α-helices adopt a near-TM orientation, in line with the "two-stage" model for membrane protein folding.[5,6]

detergent affect dimerization.[23,24] Yet, as has been pointed out by Fleming,[26] the effect of the detergent concentration can be largely eliminated, in the limit of ideal solutions, by relating the number of moles of the protein to the volume of the detergent micelles, in lieu of the total volume, which also includes the aqueous phase. The standard free energy of dissociation can then be defined in such a way that it corresponds to a 1 M concentration of detergents in water or, in the present case, to a 1 M concentration of dodecane. Adopting this convention, the apparent dissociation free energy derived from the PMF is equal to $+11.5 \pm 0.4$ kcal/mol. Extrapolating experimental data to a 1 M detergent concentration yields a dissociation free energy of +3.8 kcal/mol in dodecyldimethylaminobenzoate (C12-DMAB) micelles,[24] +5.7 kcal/mol in sodium dodecyl sulfate (SDS) micelles,[24] +7.0 kcal/mol in octylpentaoxyethylene (C8E5) micelles,[26] and +7.5 kcal/mol in C12-maltoside micelles.[24]

Although standardizing the reference state offers a more appropriate basis for comparing dissociation free energies in different media than the use of concentration-dependent equilibrium constants, a variety of other effects are also at play. For instance, the size and the shape of detergent micelles affect the orientation of the protein, and, hence, restrict the volume of the configurational space accessible to both the dimers and the monomers in ways that are not well understood. It can, nonetheless, be suggested that detergent micelles would both destabilize the dimer by imposing a stronger ordering and solvate the individual α-helices more efficiently, resulting in a dissociation free energy smaller than that in a purely nonpolar phase. In addition, the hydrophobic character of the detergent increases with the chain length and therefore seems to follow the dissociation free energy, as can be seen, for instance, in the case of C10- and C12-maltoside and C10- and C12-dimethylamine-*N*-oxide (DAO).[24] Qualitatively, the dissociation free energy in a purely hydrophobic lamellar phase is expected to be greater than that measured in detergents, albeit quantification of this difference is currently out of reach. Altogether, the lamellar arrangement of the water−dodecane environment is more similar to a water−phospholipid bilayer[44] than detergent micelles.

In comparing the present results with experiment, one should also consider statistical and systematic errors that could influence the computed free energies. One is related to the incomplete sampling of the configurational space due to slow rotational diffusion of the TM segments, especially at short and intermediate separations. This might change the depth of the PMF, although quantification of this effect is difficult. Another source of error is related to the application of periodic boundary

conditions, which, strictly speaking, yield a finite concentration PMF. At the maximum separation of the helical segments, equal to 25 Å, the distance between one α-helix and the first periodic image of the other one might also become as close as 25 Å. This, in turn, might cause concerns about artifactual electrostatic interactions between the helices. These interactions would induce a distance-dependent increase in the PMF at large separations due to unfavorable dipole−dipole interactions. This, however, is not the case. Instead, as expected, the PMF levels off at large separation, indicating that the interactions in question cannot be very strong. Since the free energy at large separations is used to anchor the PMF, possible small errors in this range would result in a small shift of the computed association free energy but would not affect the shape of the free energy profile.

The free energy contributions were calculated by partitioning the total force acting along the reaction coordinate into helix−helix and helix−solvent terms and integrating each of these forces separately. Relaxation of the individual helices and solvent reorganization are not explicit functions of ξ, but they do contribute to the free energy components indirectly. Contributions from these two effects are mainly captured in the helix−helix and helix−solvent terms, respectively. Detailed analysis of how the crossing angle, the free energy components, and the interhelical contacts vary with the reaction coordinate reveals that the mechanism of recognition and self-assembly of the TM segments of GpA is more subtle than would appear from a relatively simple free energy profile. The association process can be divided into two distinct, viz. short- and long-range, regimes. The evolution of the crossing angle formed by the α-helices with the reaction coordinate, shown in Figure 3, provides the most striking evidence for this division. Within ca. 10.5 Å, the crossing angle remains essentially constant around 43°. At this separation, which corresponds to a small "step" in the free energy profile, the TM helical segments reorient rapidly in the direction normal to the aqueous interface. This indicates that, during association, the helices move toward each other, while keeping the orientation characteristic of the monomer, as hinted by the "two-stage" model.[5,6] Only within an appreciably close distance do they form the native crossing angle.

The distinction between short- and long-range regimes is confirmed by changes in the free energy components and contacts between the α-helices (Figure 3). The global minimum in the helix−helix van der Waals term is located around 8.2 Å, which coincides with the global minimum in the PMF. As ξ increases, the close contacts in the heptad of residues responsible for interhelical association are successively disrupted between 9 and 12 Å. This leads to a rapid growth of the helix−helix free energy contribution. Interestingly, the electrostatic term is nearly constant in this interval. In contrast, the van der Waals term grows rapidly with ξ to approximately 11 Å. This means that association in the short-range regime is essentially driven by dispersive interactions.

The mechanism of association is quite different in the long-range regime. As the α-helices come together, several residues occasionally form interhelical contacts (Figure 3). Since the relative orientation of the TM segments is different from that in the dimer, the contacts are, in general, also different. Formation of these contacts is responsible for local changes in the van der Waals helix−helix contribution and in the crossing angle, which are both otherwise approximately constant. For instance, a local minimum in the van der Waals term around 15 Å corresponds to the early formation of interhelical contacts between Ile73 and Thr74, subsequently broken as additional contacts down the α-helices are formed (e.g., between Ile88 and Ile91). Beyond 18 Å, the hydroxyl moieties of Thr74 form a transient hydrogen bond, resulting in a slight increase of the average crossing angle. Although these early contacts are only intermittent and are not conserved in the native dimer, they might be viewed as recognition beacons in the dimerization process.

At large helical separations, viz. beyond 16 Å, the electrostatic helix−helix term is repulsive and decreases to zero with increasing ξ. This is an expected behavior arising from the repulsive, $1/\xi^3$, interaction of two parallel macrodipoles, ca. 80 D. Since the electrostatic contribution is negative, or nearly zero, in the short-range regime this contribution as a function of ξ necessarily goes through a maximum.

Altogether, the helix−helix term is nearly constant beyond 10.5 Å, and association is then driven almost entirely by the solvent contribution. This behavior can be understood by assuming that the formation of the solvent−protein interface is thermodynamically unfavorable. The solvent contribution reaches its global minimum near the value of ξ that separates the short- and the long-range regimes. This corresponds to a structure in which the α-helices are concomitantly in the upright position and nearly in contact. As ξ either increases or decreases, the solvent contribution increases, and so does the solvent−protein interface.

Effects of Point Mutations in Helix−Helix Association. Both replacements of Leu75 and Ile76 by an alanyl residue in the TM region of GpA result in a well-localized disruption in the interhelical association, likely to be driven by a loss of dispersion interactions that stabilize the dimer.[25] As indicated in Figure 2, these two residues are involved in long-lived interactions contributing to the overall cohesion of the helix dimer. It is important to underline that the point mutations studied here do not disrupt other interhelical contacts formed by those residues responsible for dimerization and, hence, do not affect the remainder of the structure. In a previous study,[25] replacements of Leu75 and Ile76 by alanine in the WT dimer, followed by a 1-ps MD simulation, predicted a decrease of the buried SASA of ca. 80 Å^2, an estimate that we were able to recover by a simple substitution of these residues in the absence of relaxation. In contrast, after 6 ns of "alchemical transformation", interhelical packing is optimized, so that the buried SASA does not depart significantly from its value in the WT dimer.

Configurational ensembles characteristic of contiguous intermediate states are found to overlap optimally, thereby satisfying a necessary condition for the convergence of FEP calculations.[51] The L75A and I76A "alchemical transformations" yielded a net positive free energy difference of $+1.0 \pm 0.6$ and $+1.4 \pm 0.5$ kcal/mol, respectively; the mutation free energy is equal to ΔG(dimer) $-2\Delta G$(monomer). The L75A "alchemical transformation" led to a free energy change of $+13.9 \pm 0.3$ and $+28.8 \pm 0.5$ kcal/mol, in the free and in the bound state, respectively; the I76A mutation led to a free energy change of -4.9 ± 0.3 and -8.4 ± 0.4 kcal/mol, in the single helix and in the dimer, respectively. These results fall within "chemical

(51) Lu, N.; Kofke, D. A.; Woolf, T. B. *J. Comput. Chem.* **2004**, *25*, 28−39.

accuracy" from the values determined experimentally in a micellar environment, viz. $+1.1 \pm 0.1$ and $+1.7 \pm 0.1$ kcal/mol for the L75A and I76A point mutations, respectively.[25] In contrast with the computational determination of the free energy of α-helix dimerization, the present point mutations are less dependent upon the environment, essentially because the quantity evaluated consists of a difference of free energy *differences*, thereby making the calculated and the experimental quantities directly comparable.

Concluding Remarks

The large-scale statistical mechanical simulations described here epitomize the progresses accomplished by free energy calculations in recent years and, in particular, how this methodology can be applied to capture the underlying energetics that drive the association of TM helical segments into organized, multimeric entities. To this end, the recently developed ABF scheme[35,36] has proven to constitute an appropriate and efficient strategy. The results reported in this contribution are not only in good agreement with a variety of experimental data, but also shed new light on the mechanism of recognition and association of transmembrane helices. They emphasize that association of GpA proceeds in two distinct steps. In line with the "two-stage" model of integral membrane protein folding,[4−6] it has been shown that early recognition proceeds between α-helices oriented perpendicular to the interface, suggesting that, prior to dimerization, the participating TM segments already constitute independently folded monomeric units. The second step, the formation of native contacts, is coupled to the tilt of the TM segments, resulting in the distinctive crossing angle of the tightly packed, dimeric structure. Whereas the first step in the association process is driven primarily by the solvent, the formation of the bound dimer in the second step is stabilized by helix−helix interactions, mostly of dispersive nature. In general, an improved understanding of the recognition and association processes of simple TM α-helices emerging from atomic-level computer simulations will help to decipher the folding pathways followed by more complex membrane assemblies that use recognition patterns characteristic of the prototypical GpA.[52,53]

Acknowledgment. We thank Michael A. Wilson (NASA Ames Research Center), Donald M. Engelman (Yale University), Jean-Luc Popot (IBPC, Paris), James Sturgis, and Jean-Pierre Duneau (Université d'Aix-Marseille) for fruitful discussions and helpful suggestions. The Centre Charles Hermite (CRVHP), Vandoeuvre-lès-Nancy, France, and the CINES, Montpellier, France, are gratefully acknowledged for providing generous amounts of CPU time on their SGI Origin 3800. This work was supported in part by a NASA exobiology grant to A.P.

Supporting Information Available: Complete citations for refs 33and 34. This material is available free of charge via the Internet at http://pubs.acs.org.

JA050581Y

(52) Overton, M. C.; Chinault, S. L.; Blumer, K. J. *J. Biol. Chem.* **2003**, *278*, 49369−49377.
(53) Liu, W.; Eilers, M.; Patel, A. B.; Smith, S. O. *J. Mol. Biol.* **2004**, *337*, 713−729.